

Laser-written nanoporous silicon ridge waveguide for highly sensitive optical sensors

Jinan Xia^{1,2}, Andrea M. Rossi^{2,*}, and Thomas E. Murphy³

¹Materials and Microsystems Laboratory (xLab), Politecnico di Torino, corso Duca degli Abruzzi 24, 10129 Torino, Italy

²Istituto Nazionale di Ricerca Metrologica, Strada delle Cacce 91, 10135 Torino, Italy

³Department of Electrical and Computer Engineering, University of Maryland, College Park, Maryland 20742, USA

*Corresponding author: a.rossi@inrim.it

Received October 12, 2011; revised November 29, 2011; accepted November 29, 2011;
posted November 30, 2011 (Doc. ID 155965); published January 13, 2012

We report that low-loss ridge waveguides are directly written on nanoporous silicon layers by using an argon-ion laser at 514 nm up to 100 mW. Optical characterization of the waveguides indicates light propagation loss lower than 0.5 dB/cm at 1550 nm after oxidation. A Mach-Zehnder interferometer sensor is experimentally demonstrated using the waveguide in its sensing branch, and analytical results indicate that very high sensitivity can be achieved. With large internal surface area, versatile surface chemistry, and adjustable index of refraction of porous silicon, the ridge waveguides can be used to configure Mach-Zehnder interferometers, Young's interferometers, and other photonic devices for highly sensitive optical biosensors and chemical sensors as well as other applications. © 2012 Optical Society of America

OCIS Codes: 230.7370, 160.4236, 220.4610.

Optical waveguides have been widely used for various types of high-sensitivity sensors based on photonic devices such as a Mach-Zehnder interferometer (MZI) [1], Young's interferometer [2], and a ring resonator [3]. Generally, the waveguides utilize different materials as their core layer and cladding layers, incurring different processes and techniques in the waveguide fabrication. Porous silicon has attracted interest in chemical and biological sensing due to its favorable properties: extremely high surface-area-to-volume ratio, tunable porosity, low cost, and simple fabrication. High surface-area-to-volume ratio provides a large reactive surface area in a small volume and enables more effective capture and detection of chemical and biological molecules. Particularly, a waveguide can be made from porous silicon layers that are prepared by electrochemical etching of silicon at different current densities, avoiding the deposition of different material layers. Moreover, micro/nano-optical structures for biosensors and other applications can be fabricated by rapid, low-cost, direct imprinting of porous silicon materials [4].

In this Letter, single-mode nanoporous silicon ridge waveguides are reported to be fabricated by laser direct-write technique. Light propagation loss in the waveguide is studied. The waveguide is used as a sensing element to configure a MZI sensor to mimic sensing applications. The signal output behaviors of the sensor are presented and discussed.

The waveguide was fabricated on a three-layer nanoporous silicon wafer. The porous silicon wafer was prepared by electrochemical etching of a (100) orientated p^+ -type single crystal silicon wafer with a resistivity of 8–12 m Ω cm in a solution of hydrofluoric acid, water, and ethanol in a volume ratio (1:1:2). An argon-ion laser beam at a wavelength of 514 nm was focused on the nanoporous silicon wafer, which was placed on a two-dimensional motorized stage driven by a computer. A detailed fabrication method of the optical waveguides was reported in [5]. After writing, the samples were immersed into dilute hydrofluoric acid solution to remove the oxide

produced by the laser beam. Then the samples were put into an oven for heat treatment to preoxidize waveguide structures at 500 °C for three hours. Various waveguides with widths less than 10 μ m have been made at the laser power up to 100 mW and laser scan speed up to 400 μ m/s. The waveguide as shown in Fig. 1 was fabricated at 60 mW laser power and 50 μ m/s scan speed. It was 6 mm long and 7 μ m wide. Its top cladding layer, which had a thickness of 3.3 μ m, a porosity of 72% with pore sizes ranging from 20 to 70 nm, and a refractive index of 1.5076 at the wavelength of 1550 nm, was produced by applying a current density of 440 mA/cm² to the silicon wafer. The core layer having a thickness of 3 μ m and a porosity of 70% with a refractive index of 1.5595 was formed at a current density of 400 mA/cm². The bottom cladding layer having a thickness of 8 μ m and a porosity of 72% with a refractive index of 1.5076 was produced at a current density of 440 mA/cm². The refractive indices and porosities of the porous silicon layers were obtained by fitting reflection spectra of single corresponding layers. This structural design ensures single-mode light propagation in the waveguide at a wavelength of 1550 nm.

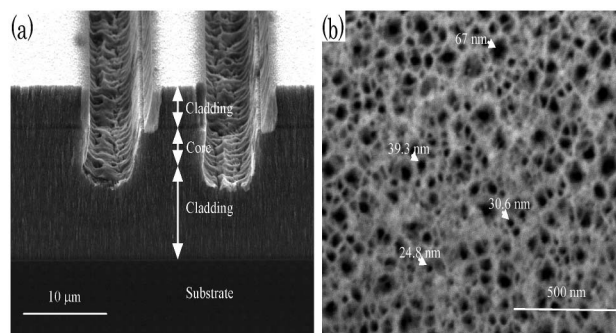


Fig. 1. Scanning electron microscope images of the waveguide: (a) cross section, (b) top view of porous silicon waveguide surface.

Light propagation loss of the ridge waveguide was measured by studying light scattering from the waveguide [6]. A laser beam was fiber-coupled into the waveguide, and the intensity of scattering light from its surface was recorded by a digital camera. Figure 2 shows a typical surface scattering light intensity distribution of the waveguide along propagation distance. The light intensity decreased exponentially with the propagation distance. In fact, the intensity of the scattered light from the surface of the sample is proportional to the intensity of guided light. From Fig. 2, the light propagation loss was obtained to be 14.7 dB/cm at a wavelength of 650 nm.

The light propagation loss is mainly attributed to Rayleigh scattering in the waveguide, rough interface scattering between guiding and cladding layers, and light absorption of porous silicon. Using the Payne-Lacey model [7,8], the maximal interface scattering loss of the waveguide at 1550 nm was calculated to be 0.01 cm^{-1} (0.04 dB/cm) with an interface roughness of 6 nm, which was measured by atomic force microscopy in the same way as reported [9]. The maximal Rayleigh scattering loss of the waveguide was inferred to be 0.45 dB/cm at the wavelength of 1550 nm based on measuring surface scattering light intensity. The light absorption of porous silicon can be ignored if the waveguide is oxidized [10]. Thus, all the light propagation loss of the waveguide at 1550 nm is lower than 0.49 dB/cm. This value is lower than the lowest reported loss in silicon-on-oxidized-porous-silicon strip waveguides [11].

As mentioned above, a waveguide can be used to configure many photonic devices for sensing applications. For this purpose, particularly for a waveguide used for a biosensor, its surface usually needs to be functionalized so that a target assay can be bound to the surface. After the assay is bound to the surface of the waveguide, the refractive index or the light propagation loss of the waveguide will change, leading to the phase shift of the light propagation through the waveguide or the change of the light output intensity of the waveguide. We used our porous silicon ridge waveguide to configure an optical sensor based on a MZI as shown in Fig. 3. We applied ethanol, methanol, cyclohexane, isopropanol, and deionized water as assays to the waveguide without surface functionalization in order to demonstrate the principle of the sensor. Light from a semiconductor laser at the wavelength of 1550 nm and the maximal power of

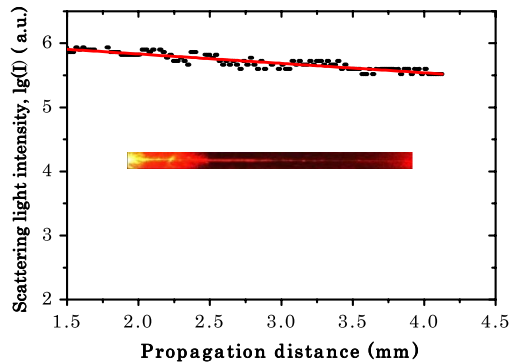


Fig. 2. (Color online) Surface scattering light intensity of a typical waveguide as a function of propagation distance. (Inset) Top view picture of scattered light along the waveguide.

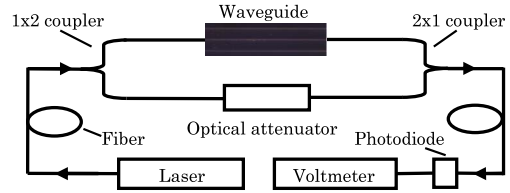


Fig. 3. Schematic diagram of experimental setup.

14 mW was split into two branches of the MZI by a 1×2 3 dB optical fiber coupler. In the reference branch there was an optical power attenuator, which balanced light powers in both reference and sensing branches. A part of light from the 1×2 fiber coupler was coupled into the waveguide in the sensing branch through a single-mode fiber. The output light of the waveguide was coupled into another single-mode fiber connected to a 2×1 optical fiber coupler. Light from the two branches of the interferometer recombined in the second optical fiber coupler, resulting in interference. The light output intensity of the second optical fiber coupler was measured by a photodiode detector, whose electrical signal was conducted to a digital voltmeter connected to a computer.

A syringe pipe was used to apply a drop of a solvent in a volume of $2 \mu\text{L}$ to the waveguide. Figure 4 shows the curves of the sensor signal intensities and change in effective index of refraction of the waveguide as a function of time after the solvents were applied to the waveguide. Initial light intensities of two branches of the MZI corresponded independently to a converted voltage of 0.162 mV measured by the photodiode detector and

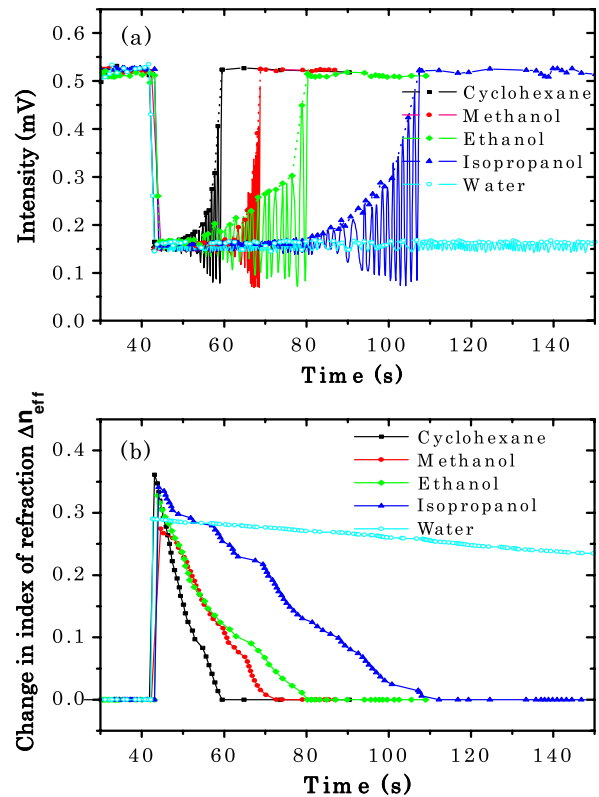


Fig. 4. (Color online) (a) Signal intensity of the sensor as a function of time. (b) Change in effective index of refraction of waveguide versus time.

the voltmeter, and the light interference intensity of the MZI was 0.523 mV as shown in Fig. 4(a). Using Eq. (1), it was obtained that the initial phase difference between two branches of the MZI was 0.405 rad:

$$I = I_1 + I_2 + 2\sqrt{I_1 I_2} \cos \Delta\Phi, \quad (1)$$

$$\Delta\Phi = \frac{2\pi L}{\lambda} (n_{\text{eff}} + \Delta n_{\text{eff}}) + \phi_0, \quad (2)$$

where I_1, I_2 are the light intensities in the reference and sensing branches, $\Delta\Phi$ the phase difference of light propagation in two branches, L the length of the waveguide, n_{eff} the effective index of refraction of the waveguide, Δn_{eff} the change of the effective index of refraction of the waveguide, λ the wavelength of the laser source, and ϕ_0 the additional phase differences induced by the two optical couplers and optical attenuator.

When a drop of a solvent was applied to the surface of the waveguide, the output light intensity of the waveguide became very weak because of both light absorption of the solvent infiltrated into the waveguide and increased light propagation loss of the waveguide, which originated in the reduction of the refractive index contrast between the core and cladding layers. The signal intensity of the sensor dropped quickly to a low value that was around the signal intensity of the reference branch as shown in Fig. 4(a). Then it fluctuated when the solvent evaporated, light absorption of the solvent and light propagation loss of the waveguide decreased, and the light output intensity of the waveguide increased. Meanwhile, the refractive index of the waveguide changed as shown in Fig. 4(b). Later, it became clear that the signal intensity of the sensor oscillated in a nonfixed period and the peak intensity increased, resulting from the phase modulation in light interference. Each oscillating cycle corresponded to a phase shift of 2π of light propagation in the waveguide.

As shown in Fig. 4(b), the index of refraction of the waveguide increased to the maximum when a drop of solvent was introduced. Then it decreased with evaporation of the solvent. A drop of cyclohexane in a volume of $2 \mu\text{L}$ evaporated within 18 s. For the same volume of methanol, it took 28 s to evaporate. For ethanol, it was 36 s, and isopropanol, 67 s. For water, it took about 8 min 30 s to evaporate, and it exhibited the same behaviors as the solvents in variations of the sensor intensity and the refractive index of the waveguide. The change in the effective index of refraction of the waveguide was obtained by measuring the phase shift that was achieved by monitoring the cycle number of the MZI signal oscillation. And it can be checked by comparing the light interference intensity of the MZI with the light intensities in the two branches. We note that a phase shift of 2π of light propagation in the waveguide corresponds to 2.58×10^{-4} in the change of effective index of refraction of the waveguide Δn_{eff} (with $L = 6 \text{ mm}$, $\lambda = 1550 \text{ nm}$), based on Eq. (2). The detection limit of Δn_{eff} for the MZI sensor is very low. If the phase resolution is $0.01 \times (2\pi)$ [12], the detection limit of refractive index change is 2.58×10^{-6} . This indicates that the MZI sensor will have very high sensitivity. However, for practical application, the setup in

Fig. 3 should be improved since we observed strong fluctuation in our measurement. Figure 4 was obtained based on data processing after removing noise, and not all the oscillations with high frequency in signal intensities modulated by large refractive index change are presented in order to show how the signals change. To improve the setup, a stable narrow-linewidth laser source, polarization-maintaining fibers, couplers, a polarization controller, and a phase compensator may be used. Another waveguide in the same silicon wafer may also be used as the reference branch instead of the fiber. Moreover, for biosensing applications, not only is surface functionalization necessary, but also the structure of the sensor needs to be modified. A fluidic channel should be formed for a liquid sample to flow on the surface of the waveguide.

In conclusion, we demonstrated that low-loss porous silicon ridge waveguides were fabricated by a low-power laser direct-write process. The laser can be replaced by many other lasers in visible wavelength range such as frequency-doubled Nd:YAG lasers and visible wavelength diode lasers, which have been widely used in industry. The low-power laser direct-write technique provides a simple and highly efficient approach to fabricate high-quality optical waveguides. We also demonstrated a Mach-Zehnder interferometric sensor in which the nanoporous silicon ridge waveguide was used as its sensing branch. This sensor has potential to provide high sensitivity. We propose that the porous silicon ridge waveguides could be used for configuring highly sensitive biological and chemical sensors based on photonic devices such as waveguides, interferometers, and other devices.

The authors thank Professor Giorgis Fabrizio for useful discussions. T. E. Murphy is supported by NSF Chemical, Bioengineering, Environmental, and Transport Systems award 0932673.

References

1. R. G. Heideman and P. V. Lambeck, *Sens. Actuators B* **61**, 100 (1999).
2. K. Schmitt, B. Schirmer, C. Hoffmann, A. Brandenburg, and P. Meyrueis, *Biosens. Bioelectron.* **22**, 2591 (2007).
3. A. Ksendzov and Y. Lin, *Opt. Lett.* **30**, 3344 (2005).
4. J. D. Ryckman, M. Liscidini, J. E. Sipe, and S. M. Weiss, *Nano Lett.* **11**, 1857 (2011).
5. A. M. Rossi, G. Amato, V. Camarchia, L. Boarino, and S. Borini, *Appl. Phys. Lett.* **78**, 3003 (2001).
6. W. Li, S. E. Webster, R. Kumaran, S. Penson, and T. Tiedje, *Appl. Opt.* **49**, 586 (2010).
7. F. P. Payne and J. P. R. Lacey, *Opt. Quantum Electron.* **26**, 977 (1994).
8. H. Schmid, A. Del age, B. Lamontagne, J. Lapointe, S. Janz, P. Cheben, A. Densmore, P. Waldron, D. X. Xu, and K. P. Yap, *Opt. Lett.* **33**, 1479 (2008).
9. P. Ferrand and R. Romestain, *Appl. Phys. Lett.* **77**, 3535 (2000).
10. P. Pirasteh, J. Charrier, Y. Dumeige, S. Haesaert, and P. Joubert, *J. Appl. Phys.* **101**, 083110 (2007).
11. E. J. Teo, A. A. Bettiol, P. Yang, M. B. H. Breese, B. Q. Xiong, G. Z. Mashanovich, W. R. Headley, and G. T. Reed, *Opt. Lett.* **34**, 659 (2009).
12. S. H. Hsu and Y. T. Huang, *Opt. Lett.* **30**, 2897 (2005).